Article

Interactions between Used Cooking Oil Biodiesel Blends and Elastomer Materials in the Diesel Engine

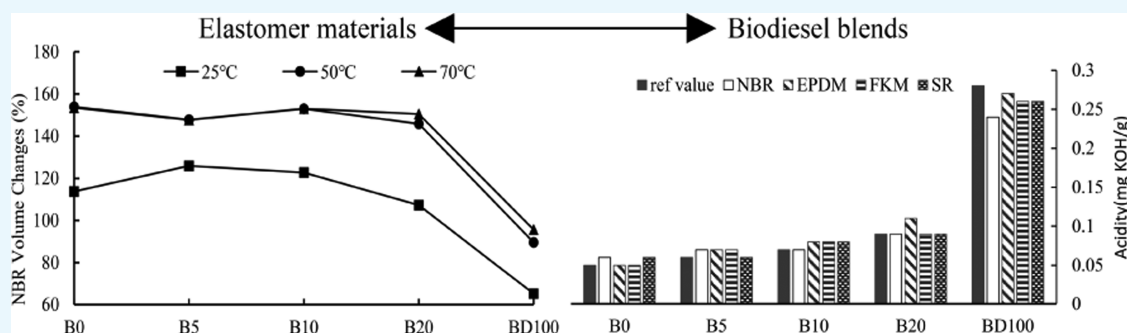Zhi-yuan Hu,* Jun Luo, Zhang-ying Lu, Zhuo Wang, Pi-qiang Tan, and Di-ming Lou

Read Online

ACCESS | Metrics & More | Article Recommendations

ABSTRACT: Used cooking oil (UCO) biodiesel may be one of the most potential alternative fuels in China to lower the dependency on crude oil for transportation. An experimental study has been conducted to assess the interactions between biodiesel produced from UCO in Shanghai and elastomer materials on high-speed marine diesel engines by immersing elastomer materials into conventional fossil diesel, 5, 10, and 20%, of a volumetric blending ratio of UCO biodiesel and pure UCO biodiesel. The test duration is 168 h at different temperatures of 25, 50, and 70 °C. Meanwhile, the effects of the mixing ratio of UCO biodiesel and the immersion temperature on the compatibility of elastomer materials with UCO biodiesel were analyzed. The results revealed that elastomer materials such as nitrile butadiene rubber (NBR), ethylene propylene diene monomer (EPDM), fluororubber (FKM), and silicone rubber (SR) exposed to biodiesel blends would reveal worse but acceptable changes than those exposed to petroleum diesel, including the slight increase of mass and volume and decline of tensile strength and hardness. FKM, NBR, and SR represented better compatibility with pure UCO biodiesel than diesel, and EPDM showed worse compatibility with UCO biodiesel as the blend ratio rises. In general, the recommended volumetric mixing ratio of UCO biodiesel should be no larger than 20%. The present study could be helpful for the investigation of UCO biodiesel blends as a potential fuel to satisfy the energy demand.

INTRODUCTION

In 2020, China's dependency on foreign crude oil reached 73.5% and the transportation industry remained in the first rank in crude oil consumption.[1] To alter the energy consumption structure in China and lower the external dependency on crude oil, utilizing some sustainable biofuels such as ethanol and biodiesel in transportation sectors is becoming increasingly prominent. Biodiesel is one of the most optimum sustainable biofuels and has been widely used in European Union (EU), Brazil, the United States (US), and some Southeast Asia countries. Moreover, Brazil, European Union, and the United States have set a probable target of 20, 10, and 25% of biodiesel blends in the total fuel consumption, respectively, by 2020.[2] The traditional feedstock of biodiesel includes soybean oil,[3] rapeseed oil,[4] palm oil[5] and other edible oils,[6] jatropha,[7] castor[8] and other nonedible oils,[9,10] and some renewable sources such as used cooking oil (UCO) and animal fats.[11] In 2019, over 33 million tons of edible oil were consumed in China, of which about 11.5 million tons are imported from foreign countries.[12] There exists no adequate edible oil to manufacture biodiesel and 20−30% of consumed edible oil becomes UCO ultimately in China, hence UCO becomes a potential raw material to produce biodiesel. The high consumption of edible oil ensures large quantities of raw materials for biodiesel, especially in densely populated cities such as Beijing, Shanghai, Shenzhen, and Chongqing. Therefore, UCO biodiesel can be used as one of the alternative transitional fuels and to reduce the dependency on crude oil in China.[13,14]
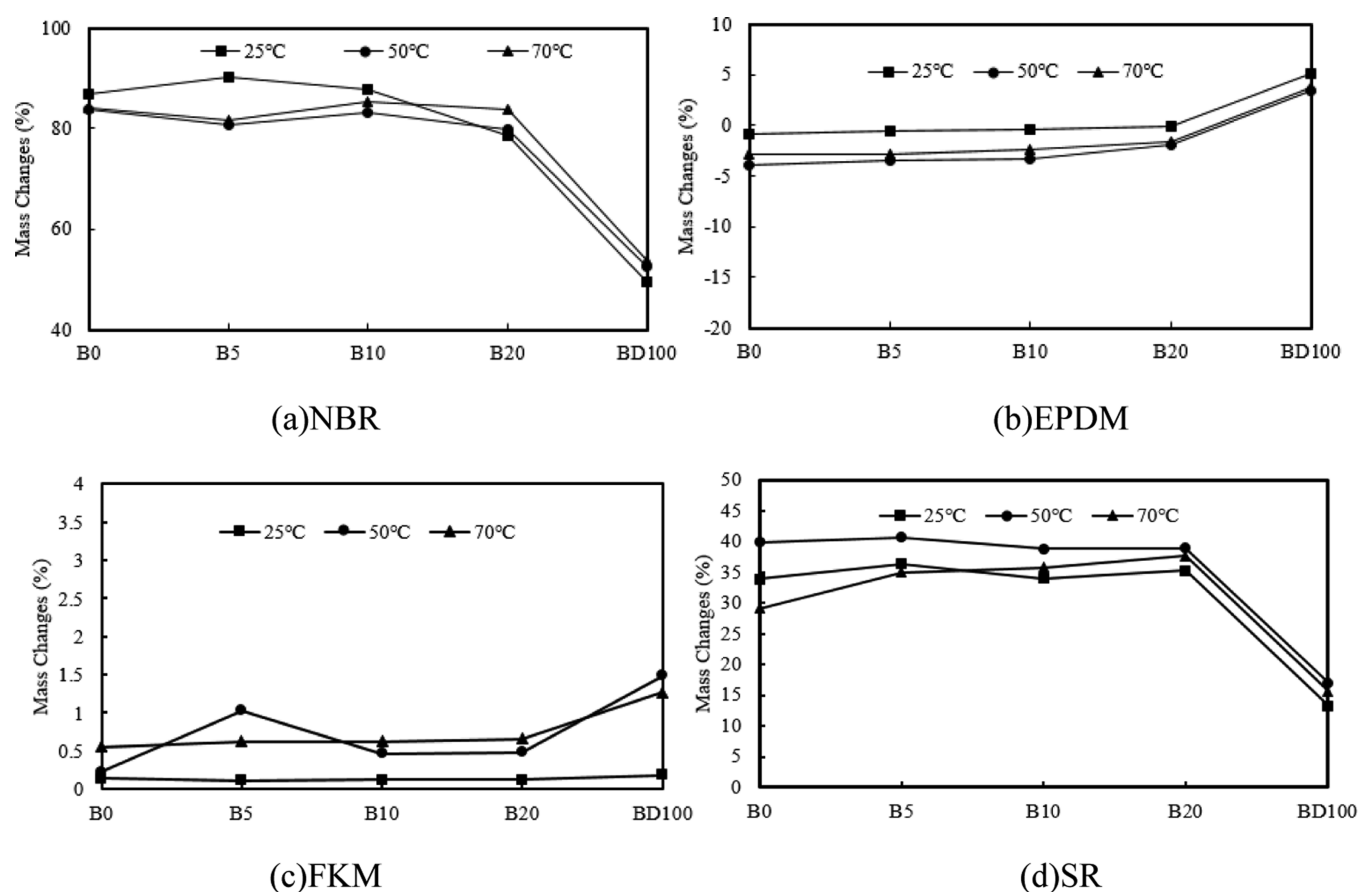
Figure 1. Mass changes of different elastomer materials after immersion.

Biodiesel consists of many C14−C20 fatty acid alkyl esters (FAMEs). The free fatty acids which are derived from the oxidation process of FAME would cause the fuel delivery elastomeric components swelling up and also could generate a series of problems including fuel line leakage, hose rupture, and seal breakage.[15,16] These problems are related with the composition and molecular structural properties of biodiesel, which could also be the major causes of the increased corrosiveness of biodiesel[17,18] and the failure of the engine parts.[19] At the same time, the properties of biodiesel blend also exhibit significant changes after the contact with the engine parts, including density, kinematic viscosity, and the total acid number.[20] Whether the biodiesel can be used in a diesel engine, an experimental study needs to be conducted to illustrate the compatibility between biodiesel and elastomer materials of the engine fuel delivery system. There have been many studies on the compatibility between materials in automotive engine fuel supply systems and single feedstock-based biodiesel, such as canola oil[21] and palm oil;[22−26] only Zhu[27] has investigated the compatibility between elastomer materials of a diesel engine and UCO biodiesel.

Most of the biodiesel compatibility studies are conducted at room temperature (25 °C). Haseeb et al.[28] studied the effects of palm oil biodiesel on the mass, volume, hardness, and tensile properties of several commonly used elastomers of diesel engines. They observed that the aforesaid properties of the ethylene propylene diene monomer (EPDM) and chloroprene rubber varied remarkably. Kass[29] assessed the compatibility of biodiesel blends with five common

elastomers using Hansen solubility parameters and found that aldehydes and short-chain acids are associated with biodiesel degradation and could further affect its compatibility with elastomers. Also, formic acid could generate higher swelling in nitrile butadiene rubber (NBR), fluorocarbon, neoprene, and silicone than what acetaldehyde did. Zhu[27] investigated the effects of the molecular structure and feedstock of biodiesel on its compatibility between biodiesel and NBR. It has been reported that the carbon chain length, number of double bonds, and alcohol moiety chain length of the fatty acid ester also have great impact on its compatibility with the NBR. Chandran[30] adopted a novel immersion method to investigate the compatibility of biodiesel with fuel delivery system materials under different diesel engine operating conditions. Compared to the typical immersion method, the new methodology can simulate the real working conditions of diesel engines including the variation of pressure and temperature, which are critical to estimate the compatibility of biodiesel with fuel delivery system materials under diesel engine working conditions.

In the fuel supply system of a diesel engine, the temperature of fuel varies greatly from the fuel tank to the fuel injector. With the deepening of research, some scholars have begun to pay attention to the compatibility of fuel system elastomer materials with biodiesel under different temperatures. Coronado[31] analyzed the resistance of nitrile rubber (NR) fuel hoses at 25 and 70 °C by utilizing gravimetric tests, tensile strength measurements, and scanning electron microscopy analysis. It has been concluded that the fuel temperature did not result in a significant mass loss of
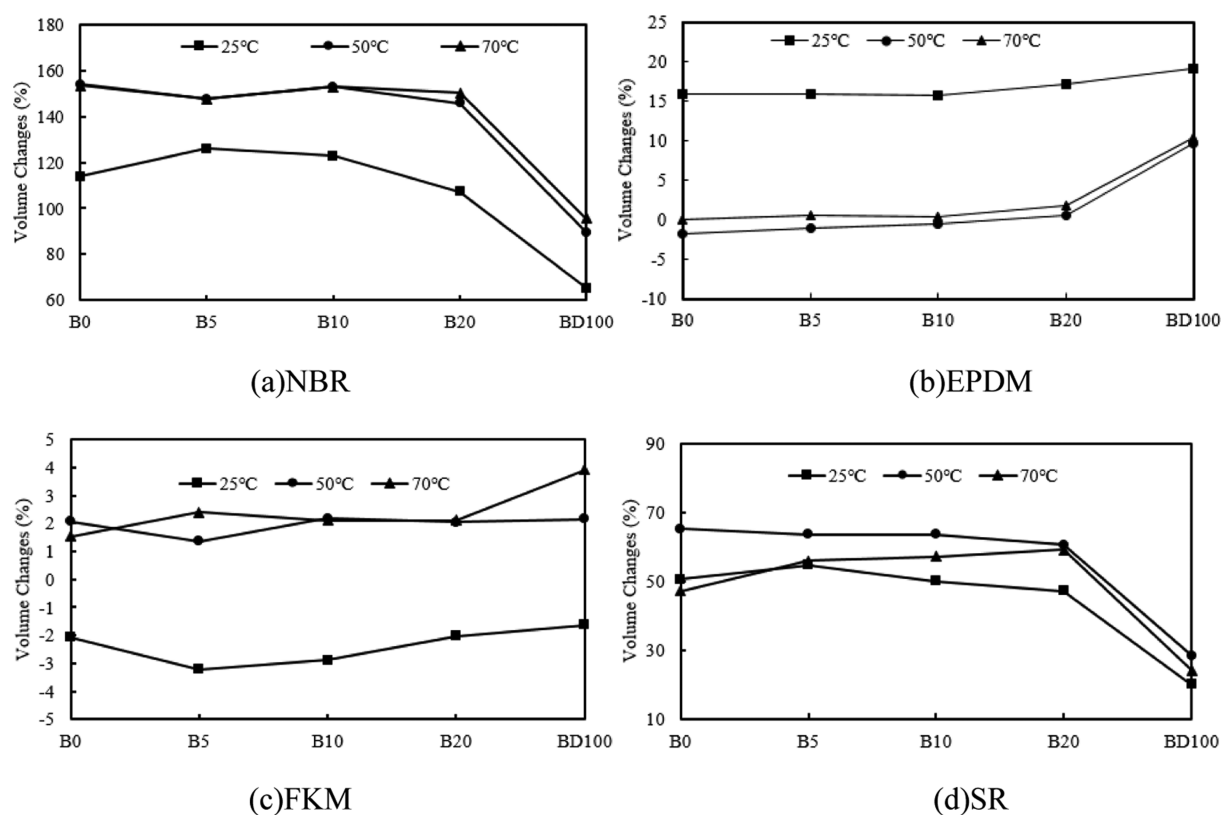
Figure 2. Changes of volume for different elastomer materials after immersion.

NR fuel hose, while the higher blend ratio of biodiesel weakened the performance of elastomers and caused the phenomenon of swelling. The exposure of hoses to different fuels with the increasing blend ratio of biodiesel led to the degradation of tensile strength. Meenakshi[32] investigated the compatibility of B0, B10, B20, and BD100 palm biodiesel blends with automotive polymeric materials including polyphthalamide and polyarylamide at 25, 50, and 70 °C. Both polymeric materials revealed a significant mass increase at higher temperature.

The components of FAMEs produced from different feedstocks are also diverse. The ingredients of UCO biodiesel are strongly dependent on the genres of UCO during the production process. There is little research about the compatibility of UCO biodiesel with elastomers at high temperature. Moreover, the blend ratio of biodiesel could be flexible for high-speed marine diesel engines according to the guidelines for marine alternative fuels of the China Classification Society.[33] Therefore, this study investigated the effects of conventional fossil diesel, three UCO biodiesel blends, that is, 5, 10, and 20%, and pure UCO biodiesels which are named as B0, B5, B10, B20, and BD100 on NBR, FKM, EPDM, and silicone rubber (SR) at 25, 50, and 70 °C, which is intended to assess the compatibility between UCO biodiesel blends and elastomer parts on high-speed marine diesel engines systematically. This study will be of help in providing valuable information for the usage of UCO biodiesel.

RESULTS AND DISCUSSION

Mass Changes. Generally, the mass of elastomer materials could be enhanced when dipped into diesel or biodiesel blends due to the diffusion effect of diesel or biodiesel. Figure 1 exhibits the mass changes of the four tested elastomer materials, that is, NBR, FKM, EPDM, and SR after being exposed to different blend ratios of UCO biodiesel at 25, 50, and 70 °C for 168 h, respectively.

Obviously, the mass of FKM was enlarged slightly as the blend ratio of UCO biodiesel increases; the EPDM reveals a slight mass decrement when the UCO biodiesel blend ratio is less than 20%, while the mass of EPDM increased remarkably in BD100. The mass of NBR and SR increased obviously when the blend ratio of UCO biodiesel is less than 20%, but the amount of increase is much smaller in BD100. Among the four tested elastomer materials, NBR was subjected to the maximal swelling, whereas FKM showed minimum swelling. According to the general principle of "like dissolves like", the polar substances in elastomers are much more likely to dissolve in polar solvents, while the nonpolar substances are more likely to dissolve in nonpolar solvents.[34] This indicates that the polarity of NBR is closer to UCO biodiesel blends, whereas that of FKM is different from UCO biodiesel. Concerning the influence of immersion temperature, as shown in Figure 1, there exist greater mass changes for NBR, EPDM, and SR at 50 than 70 and 25 °C. This can be attributed to the fact that the swelling of rubber has peaked at 50 °C. Komariah[35] has reported that the swelling of rubber will increase in the first contact of 300 h and then decrease obviously and finally remain constant at room temperature. Though the immersion time in this paper is 168 h, this phenomenon has illustrated that the higher diffusion with temperature will speed up the peak of swelling. To summarize, the swelling of engine parts can be suppressed effectively under the typical diesel engine operation conditions because the swelling of elastomer materials will be lower than the peak at higher temperature. In any case,
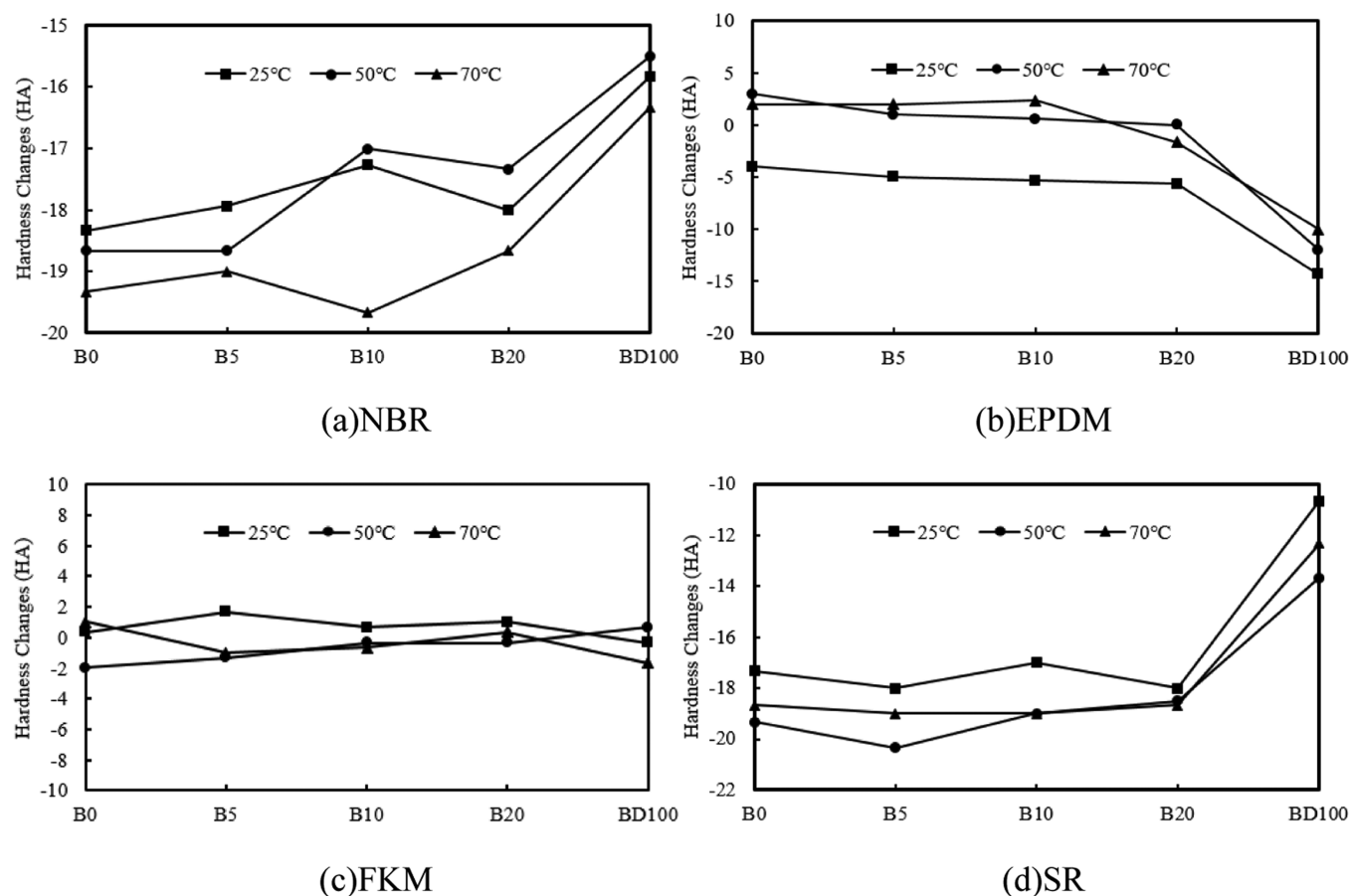
Figure 3. Changes of hardness for different elastomer materials after immersion.

the FKM may be an ideal material which can be employed in seal or pipe line systems near the injection pump.

Volume and Hardness Changes. The hardness of elastomers would be lower due to the swelling caused by biodiesel, whereas cross-linking, one of the dissolution mechanisms between biodiesel and elastomer, can inhibit this trend. Figures 2 and 3 display the volume and hardness changes of four tested elastomer materials after dipping into different test fuels at 25, 50, and 70 °C to keep the static immersion for 168 h, respectively. It can be concluded from Figures 3 and 4 that the volume of NBR and SR increased obviously and their hardness correspondingly reduced when immersed into diesel and UCO biodiesel blends. The numerical value of volume and hardness changes for NBR and SR slightly increased when the blend ratio of UCO biodiesel is less than 20% and then decreased sharply in BD100. For EPDM, the trends of volume and hardness changes were almost the same when the blend ratio of UCO biodiesel is less than 20%, and then, the volume increased moderately in BD100 but the hardness decreases obviously. For the FKM, the change of the volume and hardness waved slightly with the increase of the blend ratio of UCO biodiesel. From the perspective of volume and hardness changes, NBR was also subjected to the maximal swelling, whereas FKM showed minimum swelling compared with other tested elastomer materials.

It can be seen from Figures 2 and 3 that the value of changes for the volume and hardness is not further reduced when the immersion temperature rises from 50 to 70 °C. There is a negligible difference of volume changes for NBR,

EPDM, and FKM between 50 and 70 °C. In general, the volume reduction related to the chain softening results from chain scission and the volume increment could be attributed to the chain hardening caused by the cross-linking mechanism.[36] The dissolution of the molecular structure in the elastomer, mostly caused by the cross-linking mechanism, plays a dominant role in preventing the volume from sustainable growth, as shown in Figure 2, and causing the reduction of softening, as shown in Figure 3, even though higher temperature leads to an increase in mass. The decline of hardness for NBR, SR, and FKM is reduced with the enlargement of the blend ratio of UCO biodiesel, which means that more molecular structures are dissolved into elastomers in the form of the cross-linking mechanism instead of chain scission. For EPDM, the different performance can be attributed to the reason that the chain scission has played a more important role.

Tensile Strength Changes. Figure 4 shows the tensile strength changes of four tested elastomer materials after being exposed to different UCO biodiesel blends at 25, 50, and 70 °C for 168 h, respectively. It can be summarized from Figure 4 that the tensile strength of NBR and SR decreased deeply than EPDM and FKM upon exposure to UCO biodiesel. With the increase of the blend ratio, the degree of decline of tensile strength for NBR, SR, and FKM decreased, while EPDM reveals the opposite trend.

Among four tested elastomer materials, EPDM is nonpolar and SR, NBR, and FKM have strong polarity, thus they can absorb the solvent with similar polarity gradually by the cross-linking mechanism or chain scission. The major fatty
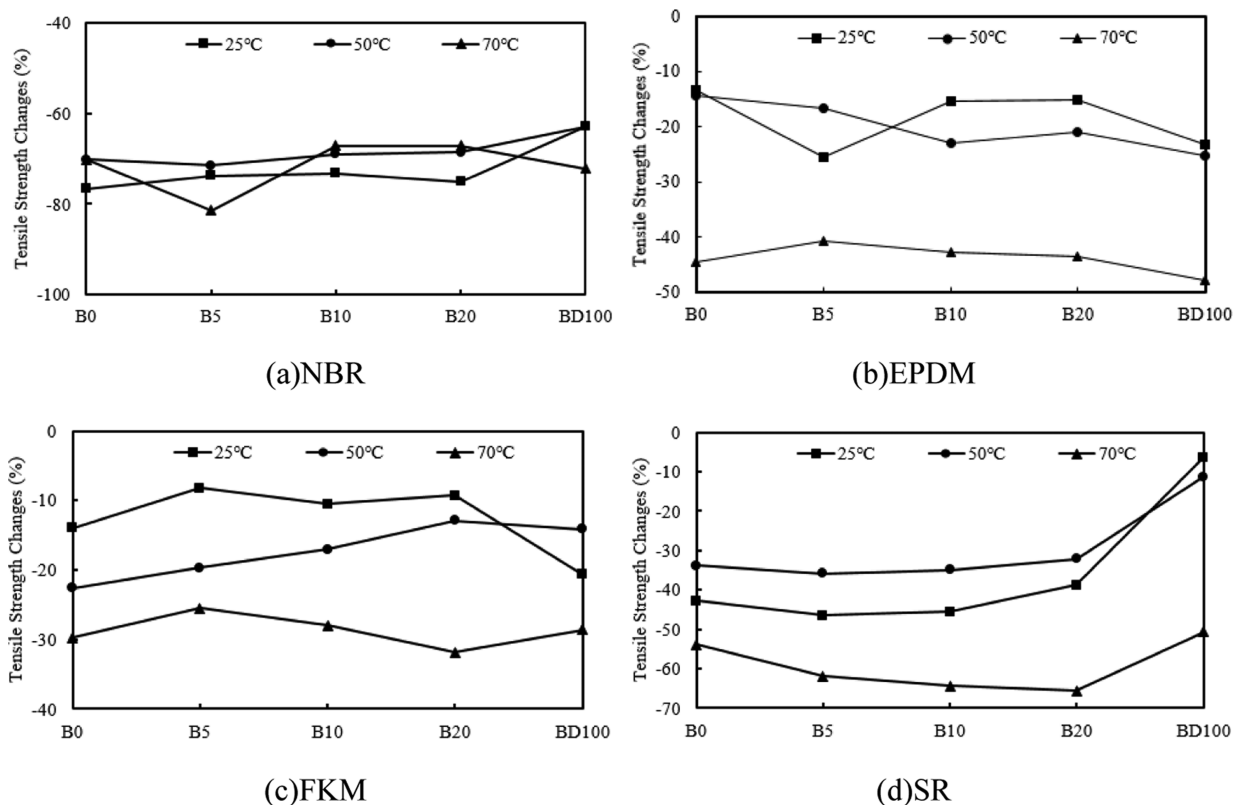
Figure 4. Changes of tensile strength for different elastomer materials after immersion.
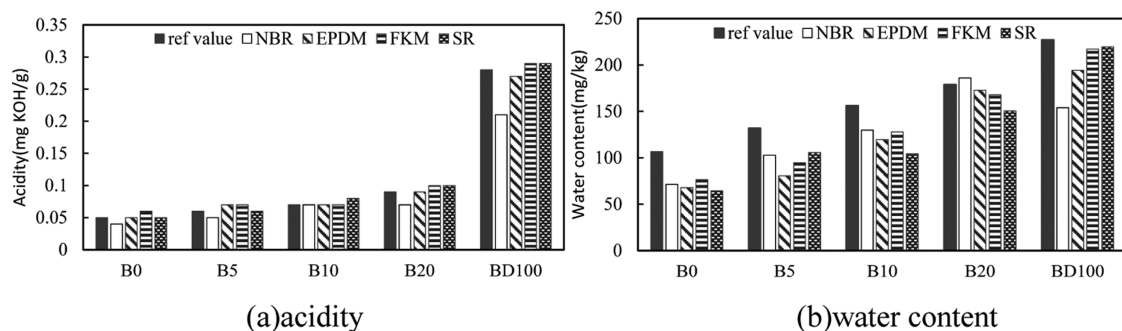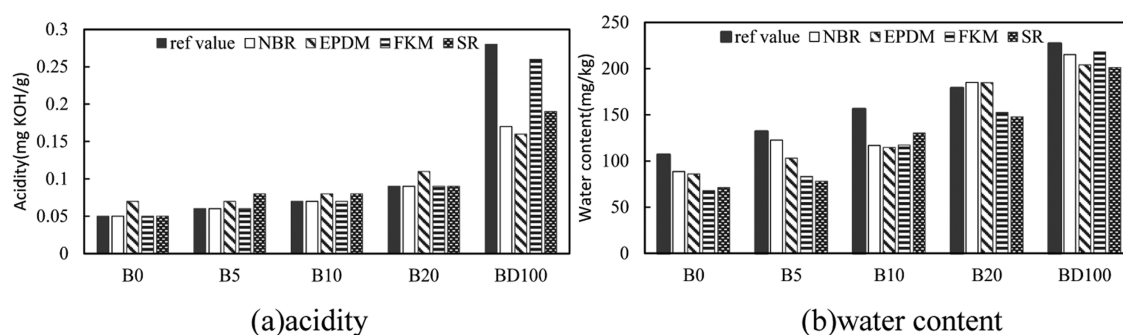

Figure 5. Changes of acidity and the water content of UCO biodiesel blends at 25 °C.

acid methyl esters of biodiesel are more easily absorbed by rubber which has similar polarity. The highest resistance to swelling for FKM could be explained by the small part of unsaturation and metal oxide/hydroxide particles in the elastomer structure.[37] Silva[38] used comprehensive multiphase (CMP NMR) to obtain information regarding the effect of biodiesel on the elastomer structure and observe the entrapped fuel into the elastomer material cavities and discovered that the higher constraint caused by the elastomer structure is related to the smaller diffusion coefficient, thereby the low diffusion coefficient of FKM may suppress the swelling. Linhares[39] also found that the choice of the accelerator occupied an important position in the resistance of the rubber to the biofuel. If the solvent−polymer interactions are more dominant than polymer−polymer interactions, maximum swelling can be obtained.[40] In short, it seems that the high mixing ratio of UCO biodiesel would not promote the decline of tensile strength for SR, NBR, and FKM.

Summary for Tested Elastomer Materials. According to the above discussions of mass, volume, hardness, and tensile strength changes of the four tested elastomer materials, that is, NBR, EPDM, FKM, and SR that are exposed to UCO biodiesel blends at different temperatures, the swelling behavior of elastomer materials is affected by the cross-linking and chain scission at the same time. The four tested elastomer materials are more easily subjected to swelling when immersed in UCO biodiesel than in diesel, especially when the blend ratio is larger than 20%. A higher temperature can also promote the swelling of elastomer materials, whereas the swelling process slowed down when the temperature further rises from 50 to 70 °C. FKM shows smaller swelling behavior than NBR, EPDM, and SR in B0, B5, B10, B20, and BD100 among all immersion elastomer materials, thus it is suitable for manufacturing any parts, particularly fuel hose, seals in fuel supply systems of high-speed marine diesel engines fueled by all blend ratios of UCO biodiesel. According to the swelling phenomenon in

Figure 6. Changes of acidity and the water content of UCO biodiesel blends at 50 °C.
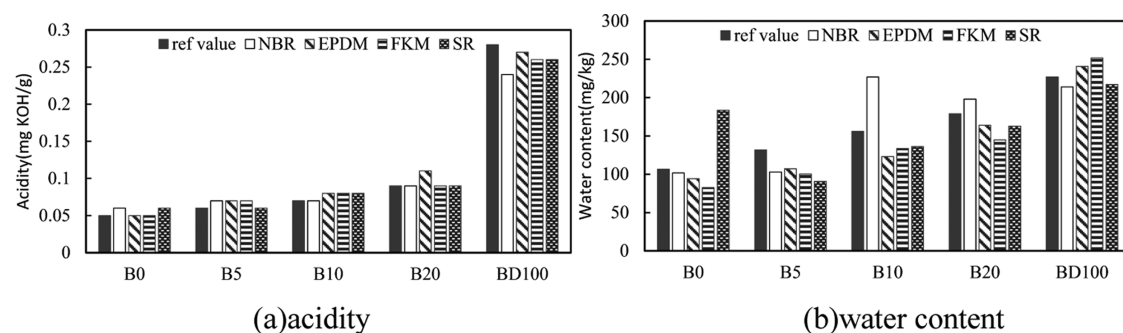
Figure 7. Changes of acidity and the water content of UCO biodiesel blends at 70 °C.

BD100 compared with B0, B5, B10, and B20, NBR and SR can be more suitable to be applied in fuel supply systems when the engine is fueled with an extremely high blend ratio of UCO biodiesel, even the pure UCO biodiesel. EPDM requires technical improvement when it is employed in a high blend ratio of UCO biodiesel due to its higher swelling in BD100.

In summary, the recommended volumetric blend ratio of UCO should not be larger than 20% when adopting no strongly antiswelling elastomer materials in the engine fuel supply system.

Fuel Property Changes. The acidity and water content of tested UCO biodiesel blends before and after the immersion test were measured to assess the impact of elastomer materials on the physical and chemical properties of the UCO biodiesel blends. Figure 5 represents acidity and water content changes of different UCO biodiesel blends exposed to NBR, EPDM, FKM, and SR at 25 °C. All the acidity and water content of UCO biodiesel blends after the immersion test were lower than the limits of diesel, B5, and BD100 standard in China. It can be concluded that the acidity of biodiesel blends decreased after the immersion test of NBR; this may be the reason why the NBR was subjected to the highest swelling after the immersion test. Also, the water content reveals a significant decrease for four elastomer materials. The diffusion of water from blends to the molecular structure of the elastomer can lower the water content.

Figure 6 represents acidity and water content changes of different UCO biodiesel blends exposed to NBR, EPDM, FKM, and SR at 50 °C. The water content still decreases almost after the immersion, which strongly supports the diffusion of water from blends to the molecular structure of the elastomer. The acidity of diesel, B5, B10, and B20 UCO biodiesel blends slightly changed after the immersion test,

and the acidity of diesel of BD100 remains significantly decreased. This may be attributed to the fact that the free fatty acid components of UCO biodiesel can be absorbed by the elastomer.

Figure 7 shows acidity and water content changes of different UCO biodiesel blends exposed to NBR, EPDM, FKM, and SR at 70 °C. The acidity of diesel, B5, B10, and B20 UCO biodiesel blends reveals moderate changes, even though the decline of acidity for BD100 is lower than that at 25 or 50 °C. This may be attributed to the fact that the higher temperature caused more hydrolysis of FAMEs. The trend of the water content still decreases for most of the immersion.

■ CONCLUSIONS

Many experimental investigations have been reported to support the potential of biodiesel. However, UCO biodiesels have not gained much importance as an easily available feedstock due to the lack of reliable scientific evidence. This paper assessed the interactions between UCO biodiesel blends and elastomer materials, that is, NBR, EPDM, FKM, and SR on high-speed marine diesel engines at different temperatures, and the effects of the mixing ratio of UCO biodiesel and immersion temperature on the compatibility of elastomer materials were analyzed. The main conclusions can be summarized as follows.

Elastomer materials such as NBR, EPDM, FKM, SR, and so forth on high-speed marine diesel engines would reveal worse but acceptable changes than those exposed to petroleum diesel, including a slight increase of the mass and volume and decline of tensile strength and hardness than that exposed to petroleum diesel when the volumetric blend ratio of UCO biodiesel is less than 20%. A higher temperature can also promote the swelling of elastomer

Table 1. Physical and Chemical Properties of Diesel and UCO Biodiesel Blends

item	test method	B0	B5	B10	B20	BD100
density (20 °C)/(kg/m^3)	ISO 3675	811.8	821.7	823.5	826.9	875.1
acidity/(mg KOH/g)	ASTM D664	0.056	0.061	0.071	0.093	0.280
sulfur/(mg/kg)	ASTM D7039	5.0	5.2	5.3	5.6	7.3
kinematic viscosity (20 °C)/(mm^2/s)	ISO 3104	3.794	4.394	4.530	4.610	4.099
water content/(mg/kg)	ISO 12937	106.6	131.8	156.1	178.8	226.9
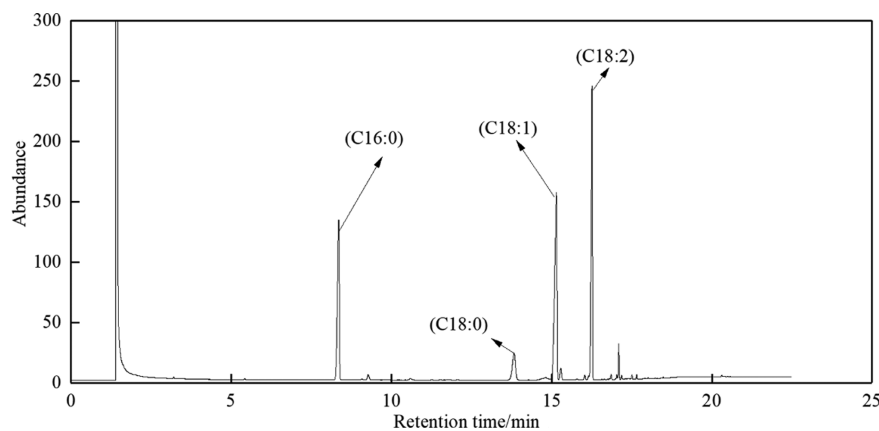
Figure 8. GC−MS analysis of UCO biodiesel in Shanghai.

materials, whereas the swelling process slowed down when the temperature further rises from 50 to 70 °C.

FKM shows better compatibility with UCO biodiesel than NBR, EPDM, and SR. The compatibility of NBR and SR with UCO biodiesel blends becomes better when the blend ratio of UCO biodiesel is high, even pure UCO biodiesel. EPDM shows poor compatibility with pure UCO biodiesel and requires technical improvement before utilizing high-speed marine diesel engines fueled with a high mixing ratio of UCO biodiesel.

There is no significant effect of elastomer materials swelling on the acidity of UCO biodiesel blends, especially when the blend ratio of UCO biodiesel is less than 20%, whereas the water content reveals a significant decrease. The recommended volumetric blend ratio of UCO biodiesel is no large than 20% when strong antiswelling elastomer materials are not utilized in the engine fuel supply system.

This paper managed to study the compatibility between elastomer materials and UCO biodiesel blends and can provide theoretical evidence to support the reliability of UCO biodiesel. Due to the complexity of UCO sources, the properties and composition of UCO biodiesel could be different in different areas. Therefore, the results obtained herein could improve casing support for theoretical discussion. The compatibility of UCO biodiesel with elastomer materials in different areas needs a further study. Future studies can be conducted by collecting the properties and composition of UCO biodiesel in other cities and areas that can provide evidence to the applicability. A relevant verification experiment can be conducted so that the results can be suitable for the UCO biodiesel in the broader region.

■ **EXPERIMENTAL SETUP AND THE PROCEDURE**

Tested UCO Biodiesel Blends. In this paper, B0, B5, B10, B20, and BD100, respectively, were selected as tested fuels. The UCO biodiesel was purchased from a company named Shanghai Zhongqi Environmental Protection Tech-

nology Co., Ltd. According to the research of Mert Gulum,[41] the influences of main transesterification reaction variables on the properties of biodiesel cannot be ignored. Transesterification reaction parameters are as follows.
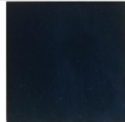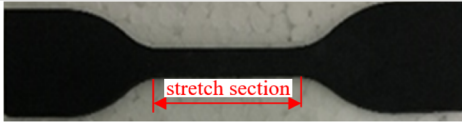
The esterified oil (acidity lower than 3 mg KOH/g, measured according to ASTM D664) after the esterification reaction is transferred to the transesterification reactor, and the methanol alkali solution is added, in which the solid KOH is 0.55−0.70% of the weight of esterified oil and methanol is 10−16% of that. The temperature of the heating reaction is controlled at 60−64 °C for 0.5−1 h. The mixture after the reaction is separated by sedimentation for 8−12 h to obtain biodiesel. The physical and chemical properties of diesel and UCO biodiesel blends are displayed in Table 1.

The feedstock of UCO biodiesel would be a mixture of different types of edible oils coming from all regions of Shanghai. The composition analysis of the tested UCO biodiesel has been investigated by gas chromatography−mass spectrometry (GC−MS) according to EN 14078. Figure 8 represents the FAME components of UCO biodiesel in Shanghai. As shown in Figure 8, UCO biodiesel in Shanghai mainly contains methyl palmitate (C16:0), methyl stearate (C18:0), methyl oleate (C18:1), and methyl linoleate (C18:2). The FAME components of UCO biodiesel were obviously different from those of biodiesel manufactured from single feedstock such as soybean, rapeseed, and palm

Table 2. Chemical Composition of Biodiesel

FAMEs	C16:0	C18:0	C18:1	C18:2	others
tested UCO	23.4	6.7	33.8	27.7	6.8
palm[42]	37.18	0.91	47.51	13.33	1.05
rice bran[42]	17.91	0.35	43.95	36.03	1.76
karanja[42]	19.48	4.90	45.99	27.77	1.86
soybean[43]	14.1	5.2	25.2	48.7	6.8
rapeseed[44]	3.73	1.8	64.84	18.47	11.16
Jatropha[45]	14.22	8.39	43.14	31.42	2.83

Table 3. Size of Square- and Dumbbell-Shaped Samples

Type	square	dumbbell
Shape		stretch section
Size	Length:25mm; Width:25mm; Thickness:2mm.	length of middle stretch section is 40mm

oil, as listed in Table 2. The unsaturated components of palm biodiesel are lower than those of other biodiesels, and the feedstock of UCO biodiesel consists of lots of waste oil in restaurant, so it can be concluded that the palm oil may be one of the major components of the UCO in Shanghai.

Tested Elastomer Materials and Immersion Temperatures. Elastomer materials were commonly used to manufacture many parts of high-speed marine diesel engines such as fuel tanks, oil pipes, fuel hoses, and seals. Among these materials, NBR, FKM, EPDM, and SR were widely used. Therefore, this research selected four elastomer materials, that is, NBR, FKM, EPDM, and SR according to ASTM D471. Each elastomer material is divided into square- and dumbbell-shaped samples, respectively. The size of square- and dumbbell-shaped samples is demonstrated in Table 3. The square-shaped sample was used to evaluate the change of mass, volume, and hardness; the dumbbell-shaped sample was used to assess the change of tensile strength.

The fuel temperature should gradually rise during the transportation process when the fuel was pumped out of the tank and supplied into the fuel injector in turn through the fuel pump, filter, hose, and pipe. Thus, this paper chose 25, 50, and 70 °C to reflect the realistic temperature of the fuel in tank, high pressure pipe, and fuel injector position, respectively, to simulate the actual temperature variation in the fuel supply system as accurately as possible.

Experimental Procedure. To assess the compatibility of four typical elastomer materials, that is, NBR, FKM, EPDM, and SR of high-speed marine diesel engines with UCO biodiesel, several static immersion tests were conducted in the case of 25, 50, and 70 °C for 168 h. The physical property changes including the mass, volume, hardness, and tensile strength would be obtained by a sample measurement before and after the immersion test. As per described in ASTM D471, a 5-decimal place analytical balance was employed to measure the mass changes and the variation of volume can be calculated by eq 1

$$\Delta V = \frac{(m_t - m_{tw}) - (m_o - m_{ow})}{m_t - m_{tw}} \times 100\% \tag{1}$$

In this formula, m_o and m_{ow} are the samples' masses in the air and water before the immersion test, while m_t and m_{tw}, respectively, correspond samples' masses in air and water after the test.

The sample hardness was measured by a durometer (model LX-A) according to ASTM D224, and tensile strength was obtained by several strength tests of the dumbbell-shaped samples with a gauge length of 30 mm on

a DLD 2500 electronic universal testing machine according to ASTM D412. In addition, acidity and the water content of the tested UCO biodiesel blends before and after the immersion test were also measured to assess the impact of elastomer materials on the UCO biodiesel blends' physical and chemical properties according to the test methods in Table 1.

■ **AUTHOR INFORMATION**

Corresponding Author

Zhi-yuan Hu − *School of Automotive Studies, Tongji University, Shanghai 201804, China;* ⓘ orcid.org/0000-0002-0906-0128; Email: huzhiyuan@tongji.edu.cn

Authors

Jun Luo − *School of Automotive Studies, Tongji University, Shanghai 201804, China*

Zhang-ying Lu − *School of Automotive Studies, Tongji University, Shanghai 201804, China*

Zhuo Wang − *School of Automotive Studies, Tongji University, Shanghai 201804, China*

Pi-qiang Tan − *School of Automotive Studies, Tongji University, Shanghai 201804, China*

Di-ming Lou − *School of Automotive Studies, Tongji University, Shanghai 201804, China*

Complete contact information is available at:
https://pubs.acs.org/10.1021/acsomega.0c06254

Notes

The authors declare no competing financial interest.

■ **REFERENCES**

(1) National Bureau of Statistics of China. Annual Data. 2021, http://data.stats.gov.cn/easyquery.htm?cn=C01 (accessed Jan 18, 2021).

(2) Acharya, N.; Nanda, P.; Panda, S.; Acharya, S. Analysis of properties and estimation of optimum blending ratio of blended mahua biodiesel. *Eng. Sci. Technol. Int. J.* **2017**, *20*, 511−517.

(3) Song, J. T.; Zhang, C. H. Comparison of performance of a diesel engine fueled with soybean biodiesel. *Appl. Mech. Mater.* **2013**, *341−342*, 1408−1411.

(4) Lešnik, L.; Biluš, I. The effect of rapeseed oil biodiesel fuel on combustion, performance, and the emission formation process

within a heavy-duty DI diesel engine. *Energy Convers. Manage.* **2016**, *109*, 140−152.

(5) Raman, L. A.; Deepanraj, B.; Rajakumar, S.; Sivasubramanian, V. Experimental investigation on performance, combustion and emission analysis of a direct injection diesel engine fueled with rapeseed oil biodiesel. *Fuel* **2019**, *246*, 69−74.

(6) Kumar, N.; Varun; Chauhan, S. R. Performance and emission characteristics of biodiesel from different origins: A review. *Renewable Sustainable Energy Rev.* **2013**, *21*, 633−658.

(7) Teo, S. H.; Islam, A.; Chan, E. S.; Thomas Choong, S. Y.; Alharthi, N. H.; Taufiq-Yap, Y. H.; Awual, M. R. Efficient biodiesel production from Jatropha curcus using CaSO4/Fe2O3-SiO2 core-shell magnetic nanoparticles. *J. Cleaner Prod.* **2019**, *208*, 816−826.

(8) Deep, A.; Sandhu, S. S.; Chander, S. Experimental investigations on castor biodiesel as an alternative fuel for single cylinder compression ignition engine. *Environ. Prog. Sustainable Energy* **2017**, *36*, 1139−1150.

(9) Banković-Ilić, I. B.; Stamenković, O. S.; Veljković, V. B. Biodiesel production from non-edible plant oils. *Renewable Sustainable Energy Rev.* **2012**, *16*, 3621−3647.

(10) Karmakar, A.; Karmakar, S.; Mukherjee, S. Properties of various plants and animals feedstocks for biodiesel production. *Bioresour. Technol.* **2010**, *101*, 7201−7210.

(11) Wang, W.; Jenkins, P. E.; Ren, Z. Electrochemical corrosion of carbon steel exposed to biodiesel/simulated seawater mixture. *Corros. Sci.* **2012**, *57*, 215−219.

(12) National Bureau of Statistics of China. *China Statistical Yearbook (2020)*: Beijing, 2020.

(13) El Shenawy, E. A.; Elkelawy, M.; Bastawissi, H. A.-E.; Panchal, H.; Shams, M. M. Comparative study of the combustion, performance, and emission characteristics of a direct injection diesel engine with a partially premixed lean charge compression ignition diesel engines. *Fuel* **2019**, *249*, 277−285.

(14) Beckman, J.; Gooch, E.; Gopinath, M.; Landes, M. Market impacts of China and India meeting biofuel targets using traditional feedstocks. *Biomass Bioenergy* **2018**, *108*, 258−264.

(15) Samuel, O. D.; Emovon, I.; Idubor, F. I.; Adekomaya, O. Characterization and Degradation of Viton Fuel Hose Exposed to Blended Diesel and Waste Cooking Oil Biodiesel. *J. Eng. Sci.* **2018**, *5*, G1−G8.

(16) Alleman, T. L.; McCormick, R. L.; Christensen, E. D.; Fioroni, G.; Moriarty, K.; Yanowitz, J. *Biodiesel Handling and Use Guide*, 5th ed.; NREL: United States, 2016.

(17) Sadrolhosseini, A. R.; Naseri, M. Investigation of Corrosiveness Biodiesel Blends Using Polypyrrole Chitosan-Cobalt/Ferrite Nanocomposite. *Prot. Met. Phys. Chem. Surf.* **2019**, *55*, 72−79.

(18) Fazal, M. A.; Jakeria, M. R.; Haseeb, A. S. M. A.; Rubaiee, S. Effect of antioxidants on the stability and corrosiveness of palm biodiesel upon exposure of different metals. *Energy* **2017**, *135*, 220−226.

(19) Nguyen, X. P.; Vu, H. N. Corrosion of the metal parts of diesel engines in biodiesel-based fuels. *Int. J. Renewable Energy Dev.* **2019**, *8*, 119−132.

(20) Samuel, O. D.; Gulum, M. Mechanical and corrosion properties of brass exposed to waste sunflower oil biodiesel-diesel fuel blends. *Chem. Eng. Commun.* **2019**, *206*, 682−694.

(21) Rocabruno-Valdés, C. I.; Hernández, J. A.; Juantorena, A. U.; Arenas, E. G.; Lopez-Sesenes, R.; Salinas-Bravo, V. M.; González-Rodriguez, J. G. An electrochemical study of the corrosion behaviour of metals in canola biodiesel. *Corros. Eng., Sci. Technol.* **2018**, *53*, 153−162.

(22) Fazal, M. A.; Haseeb, A. S. M. A.; Masjuki, H. H. Effect of temperature on the corrosion behavior of mild steel upon exposure to palm biodiesel. *Energy* **2011**, *36*, 3328−3334.

(23) Jin, D.; Zhou, X.; Wu, P.; Jiang, L.; Ge, H. Corrosion behavior of ASTM 1045 mild steel in palm biodiesel. *Renewable Energy* **2015**, *81*, 457−463.

(24) Mat, R.; Wan Nor Yuhaidi, W. N. A.; Kamaruddin, M. J.; Hassan, O. Evaluation of Palm Biodiesel−Diesel Blending Proper-

ties, Storage Stability and Corrosion Behavior. *Appl. Mech. Mater.* **2015**, *695*, 265−268.

(25) Thangavelu, S. K.; Piraiarasi, C.; Ahmed, A. S.; Ani, F. N. Corrosion Behavior of Copper in Biodiesel-diesel-bioethanol (BDE). *Adv. Mater. Res.* **2015**, *1098*, 44−50.

(26) Sa'at, N.; Samsuri, A.; Latif, N. A.; Nasir, N. F.; Madon, R. H.; Osman, S. A. Compatibility of Palm Biodiesel Blends on the Existing Elastomer Fuel Hose in Diesel Engine with Approach of Dynamic Test Rig: A Concept Study. *Mater. Sci. Forum* **2020**, *1010*, 172−177.

(27) Zhu, L.; Cheung, C. S.; Zhang, W. G.; Huang, Z. Compatibility of different biodiesel composition with acrylonitrile butadiene rubber (NBR). *Fuel* **2015**, *158*, 288−292.

(28) Haseeb, A. S. M. A.; Jun, T. S.; Fazal, M. A.; Masjuki, H. H. Degradation of physical properties of different elastomers upon exposure to palm biodiesel. *Energy* **2011**, *36*, 1814−1819.

(29) Kass, M.; Janke, C.; Connatser, R.; West, B.; Szybist, J.; Sluder, S. Influence of biodiesel decomposition chemistry on elastomer compatibility. *Fuel* **2018**, *233*, 714−723.

(30) Chandran, D.; Ng, H. K.; Lau, H. L. N.; Gan, S.; Choo, Y. M. Investigation of the effects of palm biodiesel dissolved oxygen and conductivity on metal corrosion and elastomer degradation under novel immersion method. *Appl. Therm. Eng.* **2016**, *104*, 294−308.

(31) Coronado, M.; Montero, G.; Valdez, B.; Stoytcheva, M.; Eliezer, A.; García, C.; Campbell, H.; Pérez, A. Degradation of nitrile rubber fuel hose by biodiesel use. *Energy* **2014**, *68*, 364−369.

(32) Meenakshi, H. N.; Sah, A. P.; Sah, R. Deterioration of Automotive Polymeric Materials in Exposed to Pongamia pinnata Biodiesel. *Asian J. Chem.* **2017**, *29*, 1471−1476.

(33) China Classification Society. *Guidelines for ships using alternative fuels*. 2016, https://www.ccs.org.cn/ccswzen/font/fontAction!article.do?articleId=4028e3d6571d486a0157b19b81c1021c (accessed Aug 22, 2020).

(34) Zhang, H.; Cloud, A. *Research Progress in Calenderable Fluorosilicone with Excellent Fuel Resistance*; Arlon Silicone Technologies Division, SAMPE, 2007; pp 1−7.

(35) Komariah, L. N.; Arita, S.; Aprianjaya, F.; Novaldi, M. G.; Fathullah, M. F. O-Rings Material Deterioration due to Contact with Biodiesel Blends in a Dynamic Fuel Flow. *J. Phys.: Conf. Ser.* **2019**, *1167*, 012050.

(36) Fazal, M. A.; Rubaiee, S.; Al-Zahrani, A. Overview of the interactions between automotive materials and biodiesel obtained from different feedstocks. *Fuel Process. Technol.* **2019**, *196*, 106178.

(37) Akhlaghi, S.; Pourrahimi, A. M.; Sjöstedt, C.; Bellander, M.; Hedenqvist, M. S.; Gedde, U. W. Degradation of fluoroelastomers in rapeseed biodiesel at different oxygen concentrations. *Polym. Degrad. Stab.* **2017**, *136*, 10−19.

(38) Silva, L. M. A.; Alves Filho, E. G.; Simpson, A. J.; Monteiro, M. R.; Cabral, E.; Ifa, D.; Venâncio, T. DESI-MS imaging and NMR spectroscopy to investigate the influence of biodiesel in the structure of commercial rubbers. *Talanta* **2017**, *173*, 22−27.

(39) Linhares, F. N.; Kersch, M.; Niebergall, U.; Leite, M. C. A. M.; Atlstädt, V.; Furtado, C. R. G. Effect of different sulphur-based crosslink networks on the nitrile rubber resistance to biodiesel. *Fuel* **2017**, *191*, 130−139.

(40) Eevera, T.; Rajendran, K.; Saradha, S. Biodiesel production process optimization and characterization to assess the suitability of the product for varied environmental conditions. *Renewable Energy* **2009**, *34*, 762−765.

(41) Gulum, M.; Bilgin, A. An Experimental Optimization Research of Methyl and Ethyl Esters Production from Safflower Oil. *Environ. Clim. Technol.* **2018**, *22*, 132−148.

(42) Mishra, S.; Bukkarapu, K. R.; Krishnasamy, A. A composition based approach to predict density, viscosity and surface tension of biodiesel fuels. *Fuel* **2021**, *285*, 119056.

(43) Fallen, B. D.; Pantalone, V. R.; Sams, C. E.; Kopsell, D. A.; Vaughn, S. F.; Moser, B. R. Effect of Soybean Oil Fatty Acid Composition and Selenium Application on Biodiesel Properties. *J. Am. Oil Chem. Soc.* **2011**, *88*, 1019−1028.

(44) Santaraite, M.; Sendzikiene, E.; Makareviciene, V.; Kazancev, K. Biodiesel Production by Lipase-Catalyzed in Situ Trans-esterification of Rapeseed Oil Containing a High Free Fatty Acid Content with Ethanol in Diesel Fuel Media. *Energy* **2020**, *13*, 2588.

(45) Khethiwe, E.; Clever, K.; Jerekias, G. Effects of Fatty Acids Composition on Fuel Properties of Jatropha Curcas Biodiesel. *Smart Grid Renewable Energy* **2020**, *11*, 165−180.